

Development of full particle-in-cell simulation code with adaptive mesh refinement technique

Toseo MORITAKA^{1,3)}, Masanori NUNAMI^{2,3)} and Hideyuki USUI^{1,3)}

¹⁾ Graduate school of Engineering, Kobe University, Kobe 657-8501, Japan

²⁾ National Institute of Fusion Science, Toki 509-5292, Japan

³⁾ Japan Science and Technology Agency(JST), CREST, Kawaguchi, 332-0012, Japan

(Received: 20 November 2009 / Accepted: 21 March 2010)

A numerical scheme for interface between different hierarchy levels with different grid sizes and time step intervals is designed for a full particle-in-cell simulation code with adaptive mesh refinement technique. Physical information in the interface region is exchanged recursively over all hierarchy levels. The exchange processes are performed at the synchronizing time steps with the target hierarchy level by using integer and half integer time steps in leap frog method. In addition, we employ overlap grids at the interface region in which electromagnetic field and particles are advanced under both grid conditions independently. Test simulations of light and Langmuir wave propagations indicate that the physical information can exchange smoothly through the interface region by means of the combination of these two schemes.

Keywords: multi-scale phenomena, particle-in-cell simulation, adaptive mesh refinement

1. Introduction

Full particle-in-cell (PIC) simulation[1] is a efficient simulation method to investigate microscopic plasma phenomena. Electron as well as ion kinetic properties are included in full PIC simulation and widely employed to demonstrate various phenomena in space and laboratory plasmas.

A difficulty of the PIC simulation is their considerable numerical costs. Spatial grid size and time step interval are determined by Debye length and Courant condition. These scales are usually much smaller than typical scales of plasma phenomena to be investigated. This difficulty becomes critical in multi-scale phenomena controlled by multiple plasma processes on different typical scales.

The difference of these typical scales comes from their physical origins and physical conditions. The physical origins include electron gyration motion, ion inertia, global external forces and so on. Dynamical interaction between geomagnetospheric convection driven by the global interaction with solar wind and magnetotail reconnection triggered by electron kinetic effects is a typical example of such multi-scale phenomena[2]. In addition, these typical scales are depend on the local conditions. When a simulation domain includes localized high density regions, for example, the grid size defined there by Debye length is too small to treat the surrounding environment in reasonable numerical costs. Laser induced plasma expansion is an example of such cases[3].

Adaptive mesh refinement(AMR) technique is a useful method to investigate such multi-scale phenomena. In the AMR simulation, various size grids are

dynamically applied according to the local conditions. Fine grids suitable to the local high density region are applied only there and other region is simulated by using moderate size grids. Therefore, increment of the numerical cost due to the localized region is not serious by adopting the AMR technique. The AMR technique has been rarely employed in PIC codes except for a few examples[4] while that is actively employed in fluid codes.

We have been developed a full PIC simulation code with the AMR technique in order to consider a next generation interplanetary flight system called "Magnetoplasma sail(MPS)". The propulsive force is obtained from electromagnetic interaction between solar wind and artificial magnetosphere around the spacecraft[5]. The magnetosphere is created by superconducting coils inside the spacecraft and inflated by plasma injection largely enough to interact the solar wind sufficiently. Spatial scale of the original magnetosphere is attempted to be roughly comparable to the electron gyration scale (a few kilo meters or less) and the injection plasma density could be 10^9-10^{10} times larger than the solar wind density. Therefore the solar wind interaction and the magnetic inflation for MPS are typical examples of the multi-scale phenomena to be demonstrated by means of the AMR PIC simulation.

A difficulty of the AMR technique is exchange of physical information among different hierarchy domains with different grid sizes and time step intervals. One can not reference the neighbor grids in the other hierarchies directly for finite difference scheme. Therefore an additional numerical scheme for the interface is needed for the appropriate information exchange.

author's e-mail: moritaka.toseo@cs.kobe-u.ac.jp

The outline of this manuscript is as follows; The fundamental equations to be solved in each hierarchy domain are given in Sec.2. Numerical schemes about electromagnetic field and super particles for the interface between the different hierarchy domains are explained in Sec.3 and Sec.4, respectively. These schemes are evaluated by some test simulations in each section. Conclusion and future work are described in Sec.5.

2. Fundamental equations and data structure

Basic model is a three dimensional electromagnetic explicit particle-in-cell simulation. Electromagnetic field and super particles are advanced by using leap flog method[6] for Maxwell equations

$$\mathbf{B}(n + \frac{1}{2}) = \mathbf{B}(n) - \frac{\Delta t}{2}(\nabla \times \mathbf{E}(n)) \quad (1)$$

$$\mathbf{E}(n + 1) = \mathbf{E}(n) + \frac{c^2}{4\pi} \Delta t(\nabla \times \mathbf{B}(n + \frac{1}{2})) + \mathbf{J}(n + \frac{1}{2}) \quad (2)$$

$$\mathbf{B}(n + 1) = \mathbf{B}(n + \frac{1}{2}) - \frac{\Delta t}{2}(\nabla \times \mathbf{E}(n + 1)) \quad (3)$$

and Boris-Bunemann method[1] for Newton-Lorentz equation, respectively, where n , Δt and c are time step, its interval and light speed. The charge conservation scheme[7] is employed for the local electrostatic correction in the complicated grid alignment in the AMR simulation.

The AMR simulation is structured hierarchically. Grid size and time step interval are defined according to the hierarchy levels, where high and low levels correspond to the fine and coarse grid systems, respectively. As the system evolves, some grids in a hierarchy domain (Level L) are removed according to the local physical conditions and corresponding grids in the higher hierarchy domain (Level L+1) are newly produced as the divided grids.

The dynamical grid system is organized by using fully threaded tree(FTT) structure[8]. Instead of three dimensional data matrix, the grid data is given by one dimensional array of structures which contains physical value at the grid and some pointers. The pointers represent the relationship to the other grids, such as ‘neighbor’ for the surrounding grids, ‘parent’ for the original coarse grids in the lower hierarchy and ‘child’ for the refined grids in the higher hierarchy. These relationships are varied dynamically by reconnecting the pointers.

3. Interface for electromagnetic field

3.1 Numerical scheme

Maxwell equations are solved by finite difference time domain (FDTD) method. Electromagnetic field

is advanced by referring to the neighbor grid data. However information exchange for FDTD calculation between different hierarchy levels is asynchronous due to the distinction of the time step intervals. The asynchronous information exchange could cause numerical noise at the interface because the interface region acts as an inappropriate boundary (for instance, fixed boundary for the domain with shorter time step interval).

Figure 1 shows a schematic picture of the calculation order and corresponding time steps in the hierarchy domains of levels L and L+1. Here the first integer time step and the next integer time step in level L are denoted as n and $n+1$, respectively. Field data can exchange at the integer time step in the lower level L (steps n and $n+1$ in Fig.1). Field data of lower level L at the half integer step (step $n+1/2$) also send to the higher level L+1 as the field data at integer time step by separating the calculation for electric field (Eq.2) into two steps i.e., $E(n) \rightarrow E(n + 1/2)$ and $E(n + 1/2) \rightarrow E(n + 1)$. In this way, electromagnetic field is advanced appropriately referring the field data in the other hierarchy domain except at the half integer time steps in the higher level (steps $n+1/4$ and $n+3/4$).

In addition, overlap grids are introduced at the interface region as shown in Fig.2. The electromagnetic field in the overlap grids are advanced independently in both hierarchy domains by using their own grid sizes and time step intervals. The numerical error caused at the edge of the overlap grids without the synchronized information exchange (steps $n+1/4$ and $n+3/4$) does not act on the external region until the next synchronizing time step (steps $n+1/2$ and $n+1$, respectively). The incorrect information in the overlap region is wasted and updated by the information of the other hierarchy domains in the next information exchange.

The AMR simulation with many hierarchy levels includes various time step intervals. The calculations should be made in appropriate order over all hierarchy levels. The calculations in each level are separated into two parts. The separated processes for level L are given as follows,

First half ; $B(n) \rightarrow B(n + 1/2)$, $E(n) \rightarrow E(n + 1/2)$, data exchange of $B(n + 1/2)$, $E(n + 1/2)$ with level L+1 and $E(n + 1/2) \rightarrow E(n + 1)$

Second half ; $B(n + 1/2) \rightarrow B(n + 1)$ and data exchange of $B(n + 1)$, $E(n + 1)$ with levels L-1 and L+1.

Then, the calculation order is defined recursively as follows,

← from the first half calculation of level L-1
1 calculate first half of level L

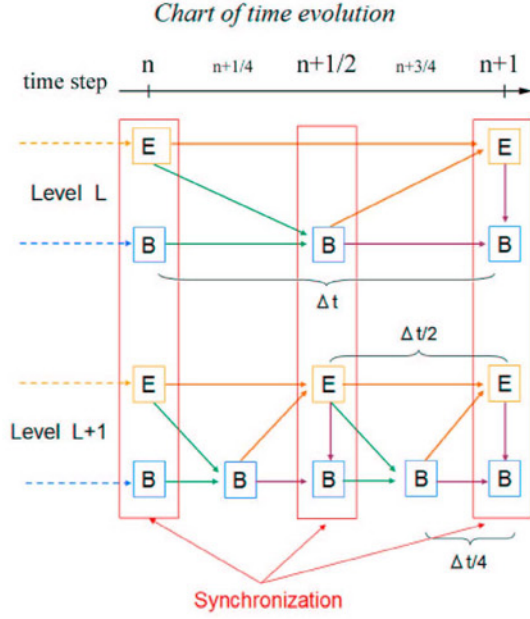


Fig. 1 Schematic of time step calculation using the leap frog method in two different hierarchy domains of level L (top) and level L+1 (bottom). The calculations flow rightward with the time evolution in this figure. Green, orange and purple arrows correspond to the calculations of $B(n) \rightarrow B(n+1/2)$, $E(n) \rightarrow E(n+1)$ and $B(n+1/2) \rightarrow B(n+1)$, respectively. Red boxes indicate synchronized data exchange processes between level L and level L+1.

- 2 → goto first half calculation of level L+1
- ← from the first half calculation of level L+1
- 3 calculate second half of level L
- goto second half calculation of level L-1.

To advance the electromagnetic field from step n to step $n+1$ in the AMR simulation with hierarchy levels $0, 1 \dots M$, we start with the first half calculation for level M (from step n to step $n+1/2^{M+1}$) and continue calculation in the above-described order until after the second half calculation for level 0. For example, the calculation order for the case of $M=2$ is obtained as,

step n : (2-1)→(2-2)→(1-1)
 →(2-1)→(2-2)→(1-2)→(0-1)
 →(2-1)→(2-2)→(1-1)
 →(2-1)→(2-2)→(1-2)→(0-2) : **step n+1**

where (m-1) and (m-2) denote the first and second half processes for hierarchy level m , respectively.

3.2 Test simulations

Test simulations of light wave propagation are performed to evaluate the numerical schemes at the interface. At initial, cosine waves of electric field $E_y(x)$ and magnetic field $B_z(x)$ in vacuum are assumed. Periodic boundary condition is employed in all directions. Spatial grids are refined according to

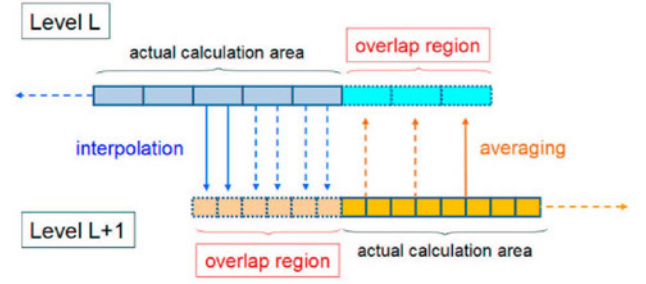


Fig. 2 Schematic of overlap region in the interface of two different hierarchy domains of level L (blue boxes) and level L+1 (orange boxes).

local magnitude of the magnetic field. Coarse (level 0), middle (level 1) and fine (level 2) grid regions are correspond to the regions with strong ($B_z \geq 0.70B_0$), moderate ($0.31B_0 \geq B_z \geq 0.70B_0$) and weak ($B_z \leq 0.31B_0$) magnetic field respectively, where B_0 is the initial amplitude of the wave. In other words, the grids are refined as the magnetic field gradient becomes steep. Theoretically, the initial wave propagates at light speed in x direction without any modification of the wave structure. The refined areas should also move with the propagating waves.

Figure 3 shows the magnetic field profiles at $t = 2.66P_0$, $3.33P_0$ and $4.84P_0$ observed in the AMR simulation using above-described interface schemes, where P_0 is the initial wave period. Blue, purple and red points denote observed magnetic field in the hierarchy domains of level 0, level 1 and level 2, respectively. The wave profile is remarkably smooth at the interface region. The wave propagates in x direction without any numerical noise.

Numerical error in the FDTD calculation about wave propagation appears as a phase error. The phase error is estimated by comparing with the theoretical wave structure. If the wave propagates at light speed without any modifications, the equation

$$B_z(x = ct, t) = B_z(x = 0, 0) = B_0, \quad (4)$$

is fulfilled. Figure 4 shows time evolutions of the $B_z(x = ct, t)$ normalized by B_0 until $t = 2.5P_0$ in three different numerical schemes for the interface region. Those are only synchronization at half integer time step (blue line), only introduction of overlap grids (green line) and both of these schemes (red line). It is shown that both of these schemes are needed to avoid the growth of the phase error modifying the wave structure.

Figure 5 is a comparison with the uniform grid case until $t = 5.0P_0$. Red line represents the profile of electric field resulting from the AMR case using both of the numerical schemes. Green and blue lines represent that resulting from the coarse and fine uniform

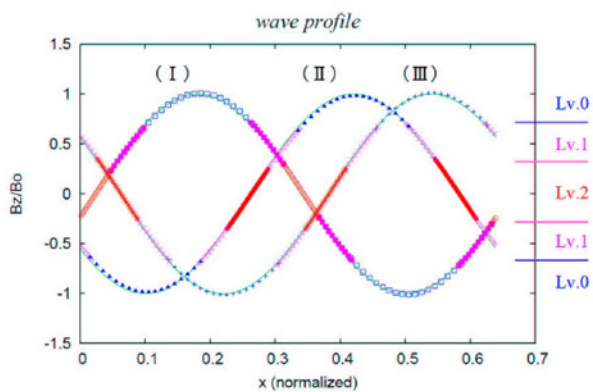


Fig. 3 Magnetic field profile in AMR case at 2.66(I), 3.33(II) and 4.84(III) periods. Grid are refined according to the local magnitude of the magnetic field B_z . Coarse grids (level 0) are refined when $B_z \leq 0.7$ and the fine grids (level 1) are refined again (level 2) when $B_z \leq 0.31$. Red line and Green lines represent initial profile and theoretical wave profiles in each time step, respectively

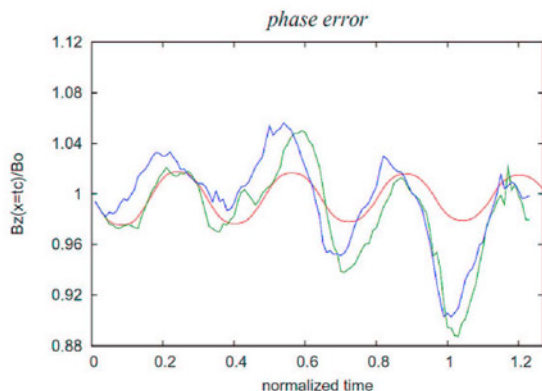


Fig. 4 Time evolutions of the magnetic field at the sampling position of $x = ct$. Blue, green and red lines represent the results of the case with the synchronization at the half integer step, with the overlap grids and with both numerical schemes, respectively.

grid cases, respectively. The grid size in the former case is the same as that of the hierarchy level 0 in the AMR case. In the uniform grid cases, the phase error increases according to the grid size but the fluctuating range is stable. The phase error in the AMR case evolves in a similar manner to that in the coarse uniform grid case at initial because sampling points $x = ct$ belong to the coarse grid area of level 0. The phase error decrease in time under the influence of the accurate wave propagation in the fine grid area. It is concluded that accuracy for the calculation of electromagnetic field with leap flog method could be enhanced without additional numerical noise by using AMR technique with the combined interface scheme of the synchronization and the overlap region.

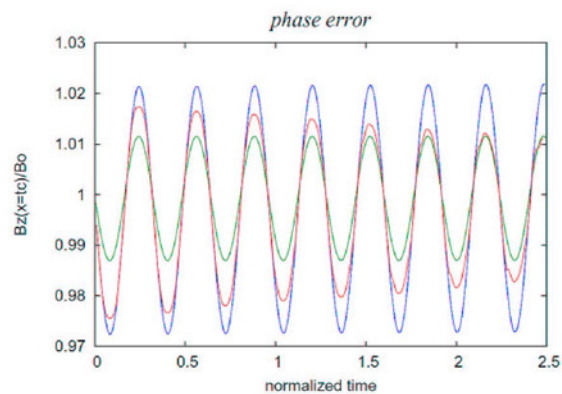


Fig. 5 Time evolutions of the magnetic field at the sampling position of $x = ct$. Red line represents the result of AMR case. Green and blue lines represent the result of uniform coarse and fine grid cases, respectively.

4. Interface region for super particles

4.1 Numerical scheme

Super particles in PIC code can move through the boundary of each hierarchy domains. In addition, neighbor grids are referred to calculate the electromagnetic force which acts to the super particles and current density due to the particle motion because the super particles have their own sizes of a few grids. Thus consistent exchange of physical information through the interface region is important in these calculation processes as in FDTD calculation of electromagnetic field.

Basic concept is same as the overlap region for electromagnetic field. That is, the physical information to be referred until the next synchronization step is ensured in the overlap grids. First, super particles near the interface are copied to the overlap region of the other hierarchy domains as shown in Fig.6. By using the copied particles, particle motion and resulting current density are calculated in each hierarchy domain independently according to their own grid sizes and time step intervals. In leap flog method, particle velocity is defined at half integer time steps. Thus velocity of the copied particles is estimated by temporal interpolation in order to synchronize the half integer time step in the destination hierarchy level.

One calculation cycle for particle motion and current density in the higher level is made without the synchronization with the lower hierarchy level as in the calculations for electromagnetic field. The overlap region should contain all grids which would be referring in these calculations. Displacement of particles during one time step is at most one grid because of the Courant condition, and surrounding one or two grids are referred to estimate the electromagnetic force acting to the particle and current density due to the

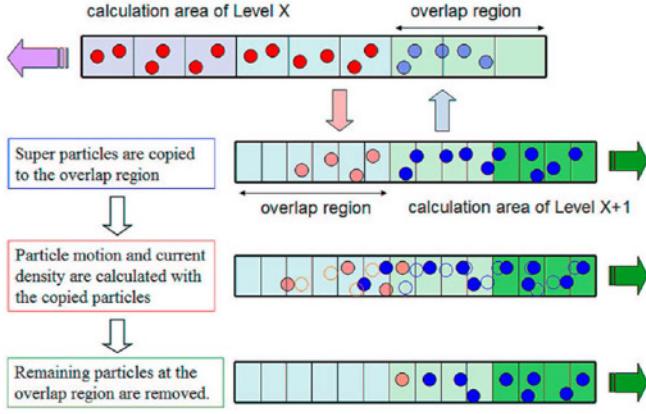


Fig. 6 Schematic picture of copy process of super particles in the overlap region. Top two figures represent the copy process between level X and level X+1. Red and blue circles indicate super particle in the hierarchy domains of level X and level X+1, respectively. Translucid circles are copied particles. Bottom two figures indicate particle motions including that of the copied particles.

displacement. Therefore width of the overlap region for the copied particles is needed to be more than two grids. These calculation is combined to the numerical scheme for electromagnetic field in the overlap region. Further overlap grids are required to calculate the time evolution of the electromagnetic field around to the particle.

4.2 Test simulations

Test simulation of Langmuir wave propagation is performed to examine the numerical scheme for electromagnetic field and super particles at the interface. Initial density, velocity and electric field profiles correspond to the Langmuir wave with a wave number k as,

$$n_e = n_0 + \tilde{n} \sin(kx) \quad (5)$$

$$E_x = \frac{2\pi\tilde{n}}{k} \cos(kx) \quad (6)$$

$$v_{ex} = \frac{\omega_{pe} E_0}{2\pi n_0 e} \sin(kx), \quad (7)$$

where E , v_e and n_e denote electric field, electron net velocity and electron density. Temperature and ion density profiles are uniform at initial. The wave number and the fluctuation of electron density are set as $k = 0.11\lambda_D^{-1}$ and $\tilde{n} = 0.1n_0$, respectively. The simulation results in the uniform grid and partially refined grid cases are compared.

Figure 7 shows the observed electric field from uniform grid case (blue lines) and partially refined case (red lines) at $t\omega_{pe} = 0.90$ (I), 2.7(II), 4.5(III) and 6.3(IV). In the latter case, grids in the range of $x/\lambda_D = 33.0$ -57.6 are refined (between two red vertical

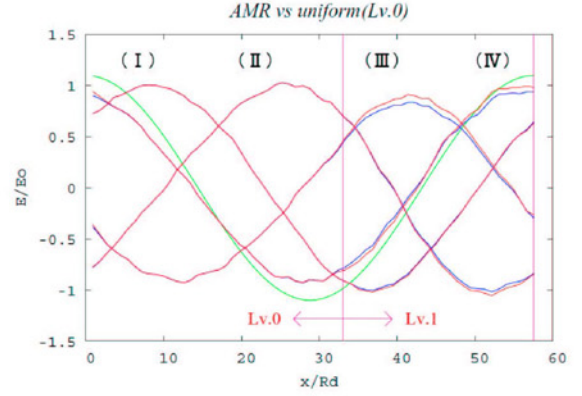


Fig. 7 Electric field profiles at $t\omega_{pe} =$ (I)0.9, (II)2.7, (III)4.5 and (IV)6.3 in the case of partially refined grid (red) and uniform coarse grid (blue). Red vertical lines represent the boundary between the coarse (left) and refined (right) grid regions in the nonuniform grid case. Green line denotes initial profile.

lines in Fig.7). The unrefined grid size is the same as the grid size in the uniform grid case. The electric field are oscillating with a period of $2\pi\omega_{pe}^{-1}$ as predicted theoretically. The profiles are almost identical in coarse grid area. Numerical error at the interface region and their influences on the other region are hardly found in the simulation results. Figure 8 is for a comparison with the uniform fine grid case. The grid size is the same as the refined grid in the nonuniform grid case. The observed electric field profiles are almost same in the fine grid area. Again numerical error is not found at the interface region.

These results indicate that physical information about plasmas and electromagnetic field can exchange consistently through the interface region by using the developed numerical scheme. However, there is slight difference between the wave amplitudes in the fine and coarse grid cases. Damping of the electric wave is found to be obvious in the coarse grids. This difference might come from the number of super particles in each grid rather than the interface scheme.

In the present scheme, total number of super particles is constant thus number of super particles per grid decreases in the fine grid. The particles number per grid can affect wave-particle interaction in phase space and resulting Landau damping. One could solve this problem by using particle revision[9] in copy process of super particles at the interface region.

5. Summary

We have developed a numerical scheme for the interface between different hierarchy levels in a full particle-in-cell simulation code with adaptive mesh refinement technique. Each hierarchy level has their own grid size and time interval. Grids in the hier-

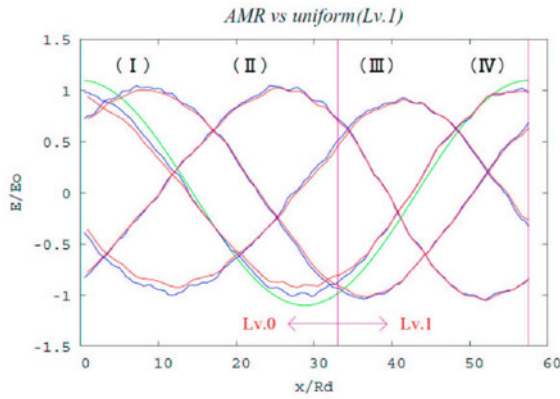


Fig. 8 Electric field profiles at $t\omega_{pe}=(\text{I})0.9$, $(\text{II})2.7$, $(\text{III})4.5$ and $(\text{IV})6.3$ in the case of partially refined grid(red) and uniform fine grid(blue). Red vertical lines represent the boundary between the coarse(left) and refined(right) grid regions in the nonuniform grid case. Green line denotes initial profile.

archy domains are removed or produced dynamically according to local physical conditions. Consistent information exchange among the different hierarchy domains is needed to avoid numerical error by adopting adaptive mesh refinement technique.

The information at the interface region is exchanged with the other hierarchy domains by using overlap grids. The electromagnetic field and super particles are copied to the overlap grids in the other hierarchy levels and advanced independently by using their own grid systems. The information exchange is performed at the synchronizing time step between different time step intervals by using integer and half integer time steps in leap flog method. Incorrect information obtained at another time step remains inside the overlap region and renewed at the next synchronization time step. The calculation order is defined recursively over all hierarchy levels.

Test simulations are performed to evaluate the validity of these numerical schemes. In the simulation of light wave propagation, phase error due to finite difference time domain calculation is reduced by using AMR technique and the interface scheme without any additional numerical noise. Langmuir waves are observed to propagate smoothly through the interface between unrefined and refined grid regions. These results suggest physical information can exchange with the other hierarchy domains consistently through the interface region by using the developed numerical scheme.

Super particles are distributed to the refined grids at the overlap region in the present copy process. Current density and number density are correctly estimated by the distributed particles. However the effective resolution of the velocity space is reduced due

to poor number of super particles per refined grid. In order to examine wave-particle interaction accurately, particle division and corresponding modification of the shape factor are needed in the next step.

Acknowledgement

This study is supported by the JST/CREST. The computation in the present study was performed with the KDK system of Research Institute for Sustainable Humanosphere (RISH) at Kyoto university.

- [1] C.K. Birdsall, and A.B. Langdon, *Plasma Physics via Computer Simulation*, (Adam Hilger, New York,1991).
- [2] A.T.Y. Lui, *IEEE Trans. Plasma Sci* **28**, 1854 (2000).
- [3] M. Nunami and K. Nishihara, *Journal of Plasma and Fusion Research SERIES* **8**, 815 (2009).
- [4] K. Fujimoto, *Physics of Plasmas* **13**, 072904 (2006).
- [5] R.M. Winglee, et al, *Journal of Geophysical Research* **105**, 67 (2000).
- [6] K.S. Yee, *IEEE Trans. Antennas Prop* **14**, 302 (1966).
- [7] T.Zh.Esirkepov, *Computer Physics Communications* **135**, 144 (2001).
- [8] A.M. Khokhlov, *Journal of Computational Physics* **143**, 519 (1998).
- [9] G. Lapenta, *Journal of Computational Physics* **181**, 317 (2002).